

Higgs Assisted Razor Search for Higgsinos at a 100 TeV pp Collider

Adarsh Pyarelal^a and Shufang Su^b

^a*School of Information, University of Arizona, Tucson, AZ 85721, USA*

^b*Department of Physics, University of Arizona, Tucson, AZ 85718, USA*

E-mail: adarsh@email.arizona.edu, shufang@email.arizona.edu

ABSTRACT: A 100 TeV proton-proton collider will be an extremely effective way to probe the electroweak sector of the Minimal Supersymmetric Standard Model (MSSM). In this paper, we describe a search strategy for discovering pair-produced Higgsino-like next-to-lightest supersymmetric particles (NLSPs) at a 100 TeV hadron collider that decay to Bino-like lightest supersymmetric particle (LSP) via intermediate Z and SM Higgs boson that in turn decay to a pair of leptons and a pair of b -quarks respectively: $\tilde{\chi}_2^0 \tilde{\chi}_3^0 \rightarrow (Z \tilde{\chi}_1^0)(h \tilde{\chi}_1^0) \rightarrow b b \ell \ell + \tilde{\chi}_1^0 \tilde{\chi}_1^0$. In addition, we examine the potential for machine learning techniques to boost the power of our searches. Using this analysis, Higgsinos up to 1.4 TeV can be discovered at 5σ level for a Bino with mass of about 0.9 TeV using 3000 fb^{-1} of data. Additionally, Higgsinos up to 1.8 TeV can be excluded at 95% C.L. for Binos with mass of about 1.4 TeV. This search channel extends the multi-lepton search limits, especially in the region where the mass difference between the Higgsino NLSPs and the Bino LSP is small.

Contents

| | | |
|----------|--|-----------|
| 1 | Introduction | 1 |
| 2 | The neutralino sector of the MSSM | 3 |
| 3 | Analysis Details | 5 |
| 3.1 | Simulation | 5 |
| 3.2 | Analysis using cut-and-count | 6 |
| 3.3 | Analysis using gradient boosted decision trees | 8 |
| 4 | Discovery and exclusion limits | 9 |
| 5 | Conclusion | 10 |

1 Introduction

The existence of dark matter provides unambiguous evidence of new physics beyond the Standard Model (SM) of particle physics. Indeed, given that there is far more dark matter in the Universe than there is baryonic matter, determining its precise nature is one of the most exciting challenges in particle physics today. One promising group of candidates for dark matter is the class of stable particles known as weakly interacting massive particles (WIMPs). These particles arise naturally in many extensions of the SM that are motivated by the need to stabilize the electroweak scale. One of the most heavily studied extensions is the Minimal Supersymmetric Standard Model (MSSM), which predicts a ‘supersymmetric partner’, or *superpartner*, for each SM particle¹. In the MSSM with R -parity conservation, the lightest supersymmetric partner (LSP) is predicted to be absolutely stable, making it a good candidate for dark matter. The identity of the LSP is determined by the mass hierarchy of the superpartners, which in turn depends on the mechanism of supersymmetry breaking. However, taking into account experimental constraints and phenomenological considerations, the lightest of the MSSM particles known as the neutralinos emerges as the most attractive candidate for the LSP [2].

Though a natural MSSM spectrum has the potential to tame the hierarchy problem, it is under siege from recent data from the Large Hadron Collider (LHC) [3, 4]. A compelling alternative scenario comes in the form of split supersymmetry (split SUSY) [5–7]. In this scenario, the lightest superpartners are the fermionic ones, on the scale of 1-10 TeV, while the scalar superpartners can be much heavier, on the scale of 100 - 1000 TeV. In exchange for accepting some level of fine-tuning, we obtain numerous benefits, including the suppression of flavor-changing neutral currents and greater compatibility with data from CP-violation

¹For a detailed review of the MSSM, see Ref. [1].

experiments. The low lying fermionic superpartners consist of neutralinos and charginos (collectively known as electroweakinos), and gluinos. The current LHC search limits on gluinos are already around 2 TeV for prompt decay and 2.5 TeV for disappearing track searches [8]. The limits on electroweakinos with heavy scalar superparticles, however, are still relatively weak: around 650 – 750 GeV or less [9–13], depending on the decay modes of the parent electroweakinos and their species. In this paper, we will focus on the discovery potential of the neutralinos and charginos at a 100 TeV pp collider.

The decay patterns of the electroweakinos (Winos, Bino, and Higgsinos) depend on the hierarchy of the MSSM parameters M_1 , M_2 , and μ ², which roughly determine the masses of the Bino, Winos, and Higgsinos, respectively [14]. In this paper, we consider the Higgsino NLSPs and Bino LSP scenario with $M_1 < \mu \ll M_2$. One of the motivations for studying Higgsinos is that the parameter μ that governs their masses plays an important role in electroweak symmetry breaking [15], and is driven to be relatively small by naturalness considerations. Finding Higgsinos has traditionally been more challenging than finding Winos, due to their smaller production rates. This, however, can be remedied by the increased production cross sections and luminosities at a 100 TeV pp collider.

Since the Bino is the only supersymmetric particle lighter than the Higgsinos in the mass hierarchy we consider, the neutral Higgsinos will decay to a Bino and a neutral SM boson (Z/h) with a branching fraction of 100%. Searches for Higgsino NLSPs with Bino LSPs via multi-lepton final states have been studied in Ref. [16] for a 100 TeV pp collider, for pair production of $\tilde{\chi}_{2,3}^0 \tilde{\chi}_1^\pm$ and $\tilde{\chi}_1^+ \tilde{\chi}_1^-$. In this paper, we attempt to exploit the relatively large branching fraction of the SM Higgs boson to b quarks, and study the potential of the $\tilde{\chi}_2^0 \tilde{\chi}_3^0 \rightarrow Zh \tilde{\chi}_1^0 \tilde{\chi}_1^0 \rightarrow bbl\ell\cancel{E}_T$ channel.

A 100 TeV pp collider would open up an immense number of physics opportunities not afforded to the 14 TeV LHC, including exploring the most interesting regions of the split SUSY parameter space [17]. Such a collider would be a natural next step after the LHC, and is being actively discussed in the particle physics community, with two major proposals being the Future Circular Collider (FCC)-hh by CERN [18], and the Super Proton Proton Collider (SppC) in China [19]. As the next energy frontier machine, it is crucial to fully explore the physics potential of a 100 TeV pp collider, especially for new particles that are either too heavy or too rare to be produced at the LHC [17, 20–22]. In particular, studies have already been performed on the prospects of discovering neutralino dark matter for compressed [23–27] and well-separated [15, 16] neutralino spectra.

In our study, we use razor variables [28], which were originally designed for searches involving two heavy, mass-degenerate pair-produced particles, each of which decays into a visible and invisible set of particles. This topology matches that of our search channel, making this set of variables a natural choice for our analysis.

At a 100 TeV collider, the SM backgrounds are going to be even larger than at the LHC. An ancillary goal of this paper is to investigate the potential for machine learning (ML) techniques to augment our analysis. With the advent of more powerful computers

²For our study, we assume all the mass parameters are positive. For the current analyses, the results do not depend much on the sign of those parameters.

and simultaneous advances in the field of statistical learning in recent years, the usage of ML is rising in experimental particle physics – in fact, the discovery of the SM Higgs boson in 2012 was done with the help of neural networks [29] and boosted decision trees (BDTs) [30].

The rest of the paper is structured as follows. In Sec. 2, we describe our model and search channel in more detail, and review the existing experimental search bounds. In Sec. 3, we describe our analysis strategies for both traditional cut-and-count analysis and analysis performed using BDTs. In Sec. 4, we present the results of our analyses, i.e. the expected 5σ discovery and 95% C.L. exclusion reaches. Finally, we conclude with the implications in Sec. 5.

2 The neutralino sector of the MSSM

The neutralino sector of MSSM consists of four mass eigenstates $(\tilde{\chi}_1^0, \tilde{\chi}_2^0, \tilde{\chi}_3^0, \tilde{\chi}_4^0)$, which are mixtures of the Bino, Wino, and two neutral Higgsinos: $(\tilde{B}^0, \tilde{W}^0, \tilde{H}_d^0, \tilde{H}_u^0)$. In the basis of these gauge eigenstates, the mass matrix of the neutralinos can be written as

$$\mathbf{M}_{\tilde{N}} = \begin{pmatrix} M_1 & 0 & -c_\beta s_W m_Z & s_\beta s_W m_Z \\ 0 & M_2 & c_\beta c_{\theta_W} m_Z & -s_\beta c_{\theta_W} m_Z \\ -c_\beta s_W m_Z & c_\beta c_{\theta_W} m_Z & 0 & -\mu \\ s_\beta s_W m_Z & -s_\beta c_{\theta_W} m_Z & -\mu & 0 \end{pmatrix}, \quad (2.1)$$

where we employ the notation $s_\theta, c_\theta = \sin \theta, \cos \theta$. Here, θ_W is the Weinberg mixing angle, and $\tan \beta = v_u/v_d$, where v_u and v_d are the vacuum expectation values of H_u^0 and H_d^0 , with $v_u^2 + v_d^2 = v^2 = (246 \text{ GeV})^2$. The parameters M_1 , M_2 , and μ are the mass parameters of the Bino, Wino, and the Higgsinos, respectively. The mass eigenstates are labeled as $\tilde{\chi}_i^0$ for $i = 1 \dots 4$ with increasing mass eigenvalues. In the limit where $m_Z \ll |\mu \pm M_1|, |\mu \pm M_2|$, the mass eigenstates are, to good approximation, a nearly pure Bino, \tilde{B}^0 , with mass M_1 , a nearly pure Wino, \tilde{W}^0 , with mass M_2 , and nearly pure Higgsinos $\tilde{H}_{1,2}^0 = (\tilde{H}_u^0 \pm \tilde{H}_d^0)/\sqrt{2}$, with mass $|\mu|$.

The optimal search strategy for finding electroweakinos highly depends on their mass spectra [14]. Phenomenological collider studies on finding electroweakinos with a small mass splitting of about 0.1 – 50 GeV at a 100 TeV pp collider can be found in [23, 25, 31, 32]. For 3 ab^{-1} of data, the projected exclusion reaches for pure Wino LSPs using the monojet channel is about 1.4 TeV. The reach can be increased to ~ 3 TeV with a disappearing tracks search. Neutralinos up to 1 TeV can be excluded for mass splittings of about 20-30 GeV, using a soft lepton search [23]. Additionally, Bino-Wino LSPs with masses up to 1.5 TeV for an inter-state mass splitting of around 1 GeV can be discovered at a 100 TeV pp collider with $\sim 7 \text{ ab}^{-1}$ of data [31].

Well-separated spectra have been studied in [15, 16] using multi-lepton channels, of the form

$$pp \rightarrow \tilde{\chi}_i \tilde{\chi}_j \rightarrow VV + \tilde{\chi}_1^0 \tilde{\chi}_1^0 \rightarrow 2\ell/3\ell + \cancel{E}_T, \quad (2.2)$$

where $\tilde{\chi}_{i,j}$ can be a neutralino or chargino, $\tilde{\chi}_1^0$ is the lightest neutralino, and V is any of the SM gauge bosons W , Z or scalar h . These searches work well since the large mass difference between the electroweakinos can lead to energetic leptons that can be easily identified. Among the multi-lepton searches for Higgsinos, the trilepton searches: $\tilde{\chi}_{2,3}^0 \tilde{\chi}_1^\pm \rightarrow WZ\tilde{\chi}_1^0 \tilde{\chi}_1^0 \rightarrow \ell\ell\ell + \cancel{E}_T$, with $\ell = e, \mu$, have the best reach, due to the relatively high production cross-section of chargino-neutralino pairs combined with the large reduction in $t\bar{t}$ and QCD backgrounds from requiring three leptons. Higgsino NLSPs can be excluded at 95% C.L. with mass up to 2.8 TeV or be discovered with mass up to 1.8 TeV, for a massless Bino LSP. The reach reduces for larger M_1 , and vanishes for $M_1 \gtrsim 600$ GeV (1000 GeV) for discovery (exclusion). Multilepton searches with Zh and ZZ as the intermediate dibosons are unlikely to be as powerful, due to the smaller pair-production cross-section of neutral Higgsinos, combined with the low branching fraction of Z/h to leptons. However, if we move beyond multilepton searches, the channel with Zh (originally suggested in Ref. [14]) as the intermediate dibosons emerges as a possible competitor to the WZ channel.

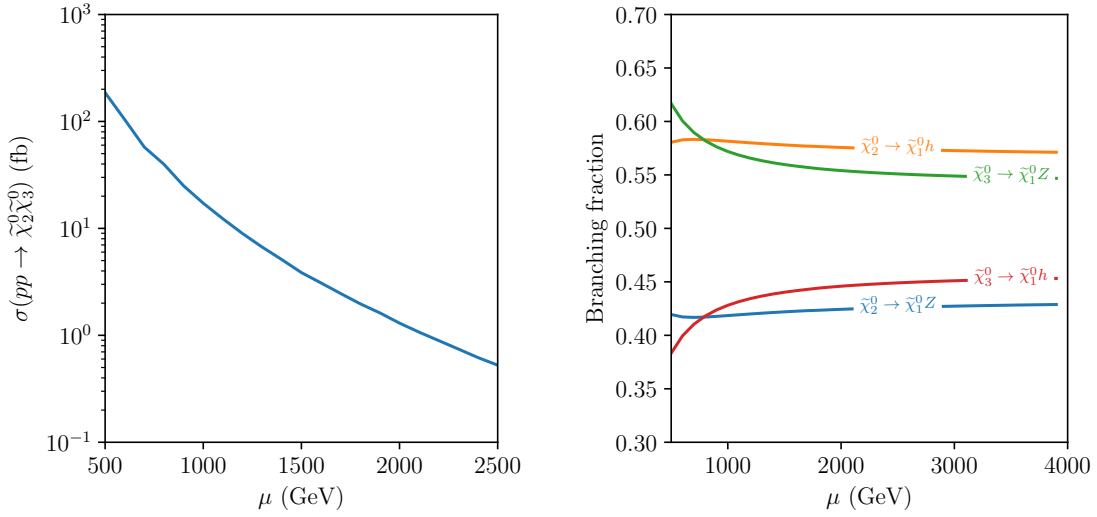


Figure 1. Higgsino pair production $\tilde{\chi}_2^0 \tilde{\chi}_3^0$ cross section (left panel), calculated using Prospino2 [33], and decay branching fractions (right panel), calculated in SUSY-HIT [34], as a function of μ for $M_1 = 25$ GeV.

In the left panel of Fig. 1, we show the pair-production cross section $\tilde{\chi}_2^0 \tilde{\chi}_3^0$ for the Higgsino-like NLSPs. The cross section varies between 200 fb to 0.5 fb for Higgsino masses between 500 GeV and 2500 GeV. The right panel of Fig. 1 shows the decay branching fractions of $\tilde{\chi}_{2,3}^0 \rightarrow Z/h\tilde{\chi}_1^0$, as calculated by SUSY-HIT [34]. While one of the Higgsinos mostly decays to Z , the other Higgsino mostly decays to h . Therefore, for pair produced Higgsinos $\tilde{\chi}_2^0 \tilde{\chi}_3^0$, the Zh mode has the greatest branching fraction. After multiplying all the branching fractions, the signal cross sections of

$$pp \rightarrow \tilde{\chi}_2^0 \tilde{\chi}_3^0 \rightarrow (Z\tilde{\chi}_1^0)(h\tilde{\chi}_1^0) \rightarrow b\bar{b}\ell\ell\tilde{\chi}_1^0 \tilde{\chi}_1^0. \quad (2.3)$$

| Stage | $\tilde{\chi}_{2,3}^0 \tilde{\chi}_1^\pm$ | $\tilde{\chi}_2^0 \tilde{\chi}_3^0$ |
|--|---|-------------------------------------|
| Pair production cross section | 60 fb | 17.2 fb |
| Intermediate diboson contribution | (WZ) 29.7 fb | (Zh) 9.15 fb |
| Applying $BR(W \rightarrow \ell\nu)$, $BR(Z \rightarrow \ell\ell)$ & $BR(h \rightarrow b\bar{b})$ | 0.42 fb | 0.37 fb |

Table 1. Comparison of Higgsino pair production cross-sections for $(\tilde{\chi}_{2,3}^0 \tilde{\chi}_1^\pm)$ and $(\tilde{\chi}_2^0 \tilde{\chi}_3^0)$, for $\mu \approx 1$ TeV, at a 100 TeV pp collider. The pair-production cross section for $\tilde{\chi}_{2,3}^0 \tilde{\chi}_1^\pm$ is taken from [16], while the pair-production cross-section for $\tilde{\chi}_2^0 \tilde{\chi}_3^0$ is calculated at Next-to-Leading Order (NLO) using Prospino2. The branching ratios to the diboson intermediate states are calculated using SUSY-HIT, and the branching fractions to the SM final states are taken from [35].

become comparable to the trilepton processes, as shown in Table 1. Thus, the $Zh + \cancel{E}_T$ signal provides an alternative discovery channel for Higgsinos. The signal contains two b -jets, two same flavor, opposite sign leptons, and missing transverse energy. The main backgrounds for this process are: $t\bar{t}$, $t\bar{b}W$ with the b and W not coming from a t , and $b\bar{b}WW$ with no intermediate s -channel top quarks.

Searches for pair produced nearly mass-degenerate Higgsinos have been performed at ATLAS and CMS for various decay topologies [11–13]. For neutralino-chargino pair production with WZ and Wh topologies, the 95% C.L. exclusion limits are about 650 GeV, 490 GeV, and 535 GeV for WZ , Wh and an equal mixture of $WZ+Wh$ topology, with the strongest limits coming from the multi-lepton searches. For neutralino pair production with ZZ , Zh , and hh topologies³, the limits are about 650 – 750 GeV via multi-lepton or multi- b jets searches, depending on the decay branching fractions of the Higgsino NLSPs.

3 Analysis Details

In this section, we describe our strategies for both the traditional cut-and-count analysis, as well as the analysis carried out with boosted decision trees.

3.1 Simulation

We simulated parton-level events using MadGraph5 v2.3.2.2 and MadEvent [36], then passed those events to Pythia 6 [37] for showering and hadronization. Finally, we used Delphes 3 [38] to perform a fast, parametrized detector simulation, with the detector card devised by the FCC-hh working group⁴. For the backgrounds, we allowed up to one additional jet in the final state, to approximate NLO QCD effects, and performed MLM matching with the `xqcut` parameter set to 40 GeV. The Higgsino pair production cross sections were calculated using Prospino2 [33] at NLO. To decouple the Wino, we set its mass parameter M_2 to 3 TeV.

³While such searches assume a gravitino LSP with Higgsino NLSPs, the limits are still relevant for our Higgsino NLSPs - Bino LSP scenario.

⁴https://github.com/HEP-FCC/FCCSW/blob/master/Sim/SimDelphesInterface/data/FCChh_DelphesCard_Baseline_v01.tcl

Since we expect our signal process to have a dilepton resonance from an on-shell Z boson, we restricted the phase space for event generation for backgrounds to the region where the invariant mass of dilepton pairs lies between 80 and 100 GeV. Additionally, the Bino dark matter that escapes the detector would result in a large amount of missing transverse energy (\cancel{E}_T), so we required a minimum \cancel{E}_T of 100 GeV at the parton level for the backgrounds as well.

At the detector simulation level, we relaxed the lepton isolation criterion in the **Delphes** detector card from ΔR_{min} from 0.4 to 0.05. This is motivated by the fact that due to the large mass difference between the Higgsino NLSPs and the Bino LSP in our search channel, the intermediate Z bosons will be highly boosted, and the leptons to which they decay will be highly collimated. The value of 0.05 is consistent with what is suggested in previous 100 TeV studies [15, 16, 31] and will allow for easier comparison between different search strategies.

3.2 Analysis using cut-and-count

For the cut-and-count analysis, we implemented successive one-dimensional cuts on the variables listed below, using the MadAnalysis 5 package [39].

1. *Trigger*: Events were selected if they had at least one lepton with $p_T^\ell > 100$ GeV.
2. *Identification*:
 - Events contain exactly two leptons of the same flavor and with opposite signs (SFOS), with $p_T^\ell > 15$ GeV and $|\eta^\ell| < 2.5$.
 - Events contain at least two b -tagged jets with $p_T^b > 30$ GeV and $|\eta^b| < 2.5$.
3. *Missing Transverse Energy*: $\cancel{E}_T > 400$ GeV.
4. *Invariant mass of Z -candidate*: $85 \text{ GeV} < m_{\ell^+\ell^-} < 95 \text{ GeV}$.
5. *Invariant mass of h -candidate*: $75 \text{ GeV} < m_{bb} < 150 \text{ GeV}$ for two leading b -jets.
6. *Razor variables*: Two razor variables are used in our analyses:

$$M_R = \sqrt{(E_Z + E_h)^2 - (p_Z^z + p_h^z)^2}, \quad (3.1)$$

$$M_T^R = \sqrt{\frac{1}{2} \left[\cancel{E}_T (|\vec{p}_{ZT}| + |\vec{p}_{hT}|) - \vec{\cancel{E}}_T \cdot (\vec{p}_{ZT} + \vec{p}_{hT}) \right]} \quad (3.2)$$

for $E_{Z,h}$ and $\vec{p}_{Z,h}$ being the reconstructed energy and momentum for Z and h , respectively. Representative kinematic distributions of these variables for a signal benchmark point with $\mu = 1$ TeV and $M_1 = 25$ GeV, as well as tt and tbW backgrounds are shown in Fig. 2, after the trigger and identification cuts. The distribution for the $bbWW$ background is not shown, since it is negligible in comparison to the others. We can see that the distribution of M_R is peaked around 1 TeV for the signal, which is consistent with what we would expect as it corresponds to the mass difference between the NLSPs and the LSP. The tt background peaks around 500 GeV, while the distribution of tbW background almost overlaps with that of the signal process. Similar behaviour is also seen in the M_T^R distributions. For this mass combination, requiring $M_R > 800$ GeV and $M_T^R > 400$ GeV yields the greatest significance.

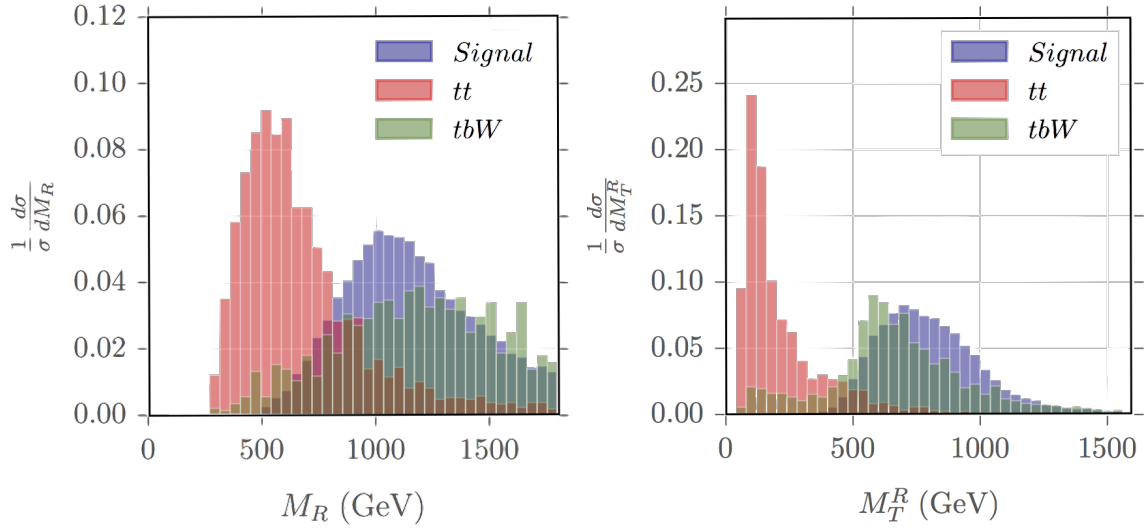


Figure 2. Normalized distributions of the razor kinematic variables M_R (left) and M_T^R (right) for a signal benchmark point with $\mu = 1$ TeV and $M_1 = 25$ GeV, as well as the dominant tt and tbW backgrounds after the trigger and identification cuts.

| | σ_{signal} | $\sigma_{t\bar{t}}$ | σ_{tbW} | σ_{bbWW} | $\sigma_{BG} (total)$ | S/B | S/\sqrt{B} |
|-----------------------------|-------------------|---------------------|----------------|----------------------|-----------------------|----------------------|--------------|
| Original | 0.37 | 35,998 | 4,176 | 7.8 | 40,182 | 9.1×10^{-6} | 0.10 |
| Trigger | 0.31 | 5,321 | 1,058 | 2.5 | 6,382 | 4.9×10^{-5} | 0.21 |
| SFOS leptons | 0.25 | 1,774 | 360 | 0.88 | 2,135 | 1.2×10^{-4} | 0.30 |
| 2 b jets | 0.04 | 290 | 62 | 0.09 | 352 | 1.3×10^{-4} | 0.13 |
| $\cancel{E}_T > 400$ | 0.03 | 5.3 | 6.8 | 0.007 | 12 | 0.003 | 0.49 |
| $m_{\ell\ell} \in [85, 95]$ | 0.03 | 2.1 | 3.3 | 0.004 | 5.3 | 0.005 | 0.62 |
| $m_{bb} \in [75, 150]$ | 0.02 | 0.59 | 0.30 | 8.2×10^{-4} | 0.90 | 0.02 | 1.3 |
| $M_R > 800$ | 0.02 | 0.03 | 0.20 | 3.3×10^{-4} | 0.23 | 0.09 | 2.2 |
| $M_T^R > 400$ | 0.02 | 0.008 | 0.18 | 1.9×10^{-4} | 0.19 | 0.10 | 2.4 |

Table 2. Representative cut flow table for a signal benchmark point with $\mu = 1$ TeV, $M_1 = 25$ GeV at 100 TeV pp collider, for a traditional cut-and-count analysis. All cross sections are given in unit of fb, and the units for the missing energy, invariant mass, and razor variable cuts are GeV. The significance, S/\sqrt{B} , is calculated for an integrated luminosity of 3 ab^{-1} .

Table 2 shows the cut efficiencies for a representative signal benchmark point with $\mu = 1$ TeV and $M_1 = 25$ GeV. The cross-sections of the backgrounds are obtained from MadEvent after performing the MLM matching procedure. Their small size reflects the $m_{\ell\ell}$ and \cancel{E}_T cuts we imposed at the parton level. For all the benchmark points, we require a minimum of 3 signal events left over after cuts. We can see that, after applying our cuts, tbW remains as the dominant backgrounds, followed by tt . The values of the razor variable cuts were chosen to maximize the significance, S/\sqrt{B} (calculated for an integrated luminosity of 3000 fb^{-1}), shown in the last column.

3.3 Analysis using gradient boosted decision trees

For each signal mass combination and each background process, we preselected events that passed the lepton trigger, contained two SFOS leptons and two b -tagged jets, and calculated a number of kinematic variables for each event. We then placed these kinematic variables in an array, with each row corresponding to an event, and the columns corresponding to the kinematic variables. A mixture of low-level and high-level kinematic variables was shown to have the greatest effectiveness. The kinematic variables chosen were $m_{\ell\ell}$, m_{bb} , M_R , M_T^R , \cancel{E}_T , the total hadronic transverse energy H_T , and the transverse momenta of individual final state leptons and b -quarks: $p_T^{\ell_1}$, $p_T^{\ell_2}$, $p_T^{b_1}$, and $p_T^{b_2}$. We then divided the generated events into training and test sets, with the training set comprising 75% of signal events and 30% of background events. We used the `scikit-learn` package [40] to implement our analysis. A boosted decision tree classifier was trained with 1000 weak learners and a learning rate of 0.025.

After the classifier is trained, we use it to assign scores to individual events. A more negative score indicates a more background-like event, and a more positive score denotes a more signal-like event. After the scores have been assigned to the events in the test sets, we can use this score just as we would a regular kinematic variable, that is, we apply a cut that selects events with a minimum of this score. The value of the cut is chosen to maximize the significance for each signal benchmark point. The distribution of scores for the representative benchmark point ($\mu = 1$ TeV, $M_1 = 25$ GeV) is shown in Fig. 3. We observe that there is an appreciable separation between the signal and background distributions.

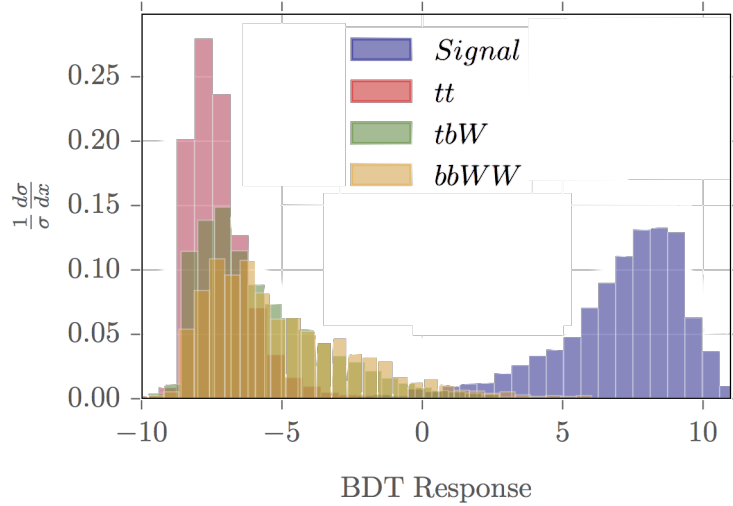


Figure 3. Distribution of the decision function of the gradient boosted decision tree classifier for the representative signal benchmark point ($\mu = 1$ TeV, $M_1 = 25$ GeV) and backgrounds.

Table 3 shows the cut efficiencies for the same representative benchmark point as in Table 2, but this time for a boosted decision tree analysis. We observe that the statistical significance we can achieve goes up from 2.4 to 8.4, a roughly four-fold increase.

| | σ_{signal} | $\sigma_{t\bar{t}}$ | σ_{tbW} | σ_{bbWW} | $\sigma_{background\ (total)}$ | S/B | S/\sqrt{B} |
|--------------------|-------------------|---------------------|----------------|-----------------|--------------------------------|---------|--------------|
| Original | 0.37 | 35,998 | 4,176 | 7.8 | 40,182 | 9.1e-06 | 0.10 |
| Preselection | 0.04 | 290 | 62 | 0.09 | 352 | 1.3e-04 | 0.13 |
| BDT response > 5.1 | 0.04 | 0.02 | 0.04 | 4.8e-04 | 0.06 | 0.63 | 8.4 |

Table 3. Representative cut flow table for the same benchmark point and integrated luminosity as in Table 2, but using a BDT analysis instead. The preselection is equivalent to the trigger and identification cuts listed in Table 2. As before, all the cross sections are in fb.

For certain values of the cuts on kinematic variables or the score of the classifier, no events survived for one or more of the background components. To guard against overly optimistic estimates of the significance S/\sqrt{B} , we set a lower bound of 3 for the number of Monte Carlo (MC) events after cuts for each background component, corresponding to the 95% confidence interval for a Poisson distribution.

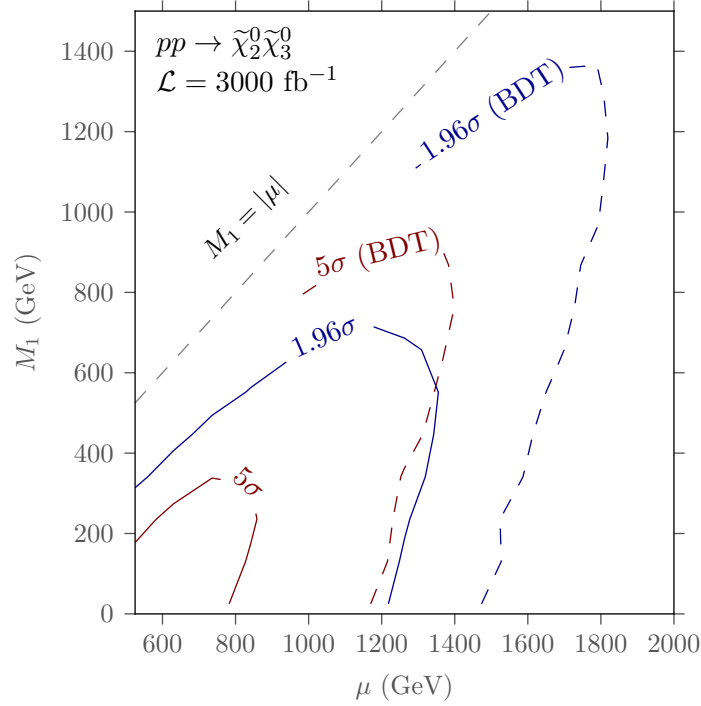


Figure 4. Discovery (red) and exclusion (blue) contours for the traditional cut-and-count analysis (solid) and boosted decision tree analysis (dashed), for 100 TeV pp collider with an integrated luminosity of 3000 fb^{-1} .

4 Discovery and exclusion limits

Fig. 4 shows the expected reach for 95% C.L. exclusion and 5σ discovery in the parameter space of μ vs. M_1 for 100 TeV pp collider with an integrated luminosity of 3000 fb^{-1} . The

cut-and-count strategy is able to discover Higgsinos up to 850 GeV and exclude them up to 1.35 TeV. The boosted decision tree analysis improves this reach – it is able to discover Higgsinos up to 1.4 TeV, and exclude them up to 1.8 TeV in favorable points in parameter space. Similarly, Binos can be discovered up to 350 GeV and excluded up to 700 GeV with the rectangular cut analysis, and the BDT analysis can discover them up to about 900 GeV and exclude them up to 1.4 TeV. Since the background left after cuts is relatively low, we do not include systematic errors in these estimates.

Comparing the BDT results with that of the cut-and-count bases analysis, the improvement is substantial, but perhaps not spectacular. However, it should be kept in mind that this is probably a conservative estimate. Since we reserve 30% of the background data for training purposes, and impose the condition that the minimum number of MC events after cuts for the backgrounds must be 3, the true rate of background rejection by the classifier is likely underestimated, and the expected significance from the BDT analysis will improve. This extrapolation is qualitatively supported by the high degree of separation between signal and backgrounds seen in Fig. 3, and the fact that a larger fraction of the signal events are preserved with the BDT approach compared to the rectangular cut approach, as can be seen in Tables 2 and 3.

In regions with large mass differences between the LSP and NLSP, the reach in μ is reduced. This is because the intermediate SM Higgs boson will be highly boosted, and thus decay into a highly collimated pair of b -jets. The extent to which this affects our results can be estimated from Table 2. We see that requiring two b -tagged jets reduces our signal cross-section by roughly 87%. This is far more than the 28% reduction that one might naively expect as a result of applying the b -tagging efficiency of about 85% specified in our `Delphes` card.

For massless Binos, the reach of the $Zh + \cancel{E}_T$ channel in our study is less than the reach of the multi-lepton channel studied in Ref. [16], which can exclude Higgsinos with masses up to 2.8 TeV and discover them for masses up to 1.8 TeV. However, for heavier Binos (larger M_1), the reach of the multi-lepton channel is reduced, and vanishes completely for $M_1 \gtrsim 600$ GeV (1000 GeV) for discovery (exclusion). In this region, the reach of the $Zh + \cancel{E}_T$ channel in our study exceeds that of the multi-lepton search for larger LSP masses: an increasement of about 300 GeV with BDT analysis.

5 Conclusion

In this paper, we examined the discovery/exclusion potential of a 100 TeV pp collider for pair-produced heavy Higgsino NLSPs with a Bino LSP, via intermediate Z and h bosons that decay to a pair of leptons and b quarks respectively: $\tilde{\chi}_2^0 \tilde{\chi}_3^0 \rightarrow Zh \tilde{\chi}_1^0 \tilde{\chi}_1^0 \rightarrow bbl\ell\ell\cancel{E}_T$.

We pursued two analysis strategies. One was the traditional cut-and-count methods, including razor variables that are sensitive to the mass difference between the LSP and the NLSPs. The other strategy was to use a boosted decision tree classifier trained with a number of low- and high-level kinematic variables, including razor variables. We expected that the machine learning approach would be able to more efficiently determine the optimal decision

boundary between signal and background events in feature space than the traditional cut-and-count method.

Overall, we find that the reach of our analysis strategy is a significant improvement over that of the LHC. We found that the rectangular cut strategy has the potential to discover Higgsino NLSPs up to a mass of 850 GeV, and exclude them up to a mass of 1.35 TeV, for a Bino LSP mass around 350 GeV and 700 GeV respectively. As expected, the boosted decision tree classifier performs better, with the ability to discover Higgsino NLSPs up to 1.4 TeV and exclude them up to a mass of 1.8 TeV, for a Bino mass of about 900 GeV and 1.4 TeV respectively. In the process, we highlighted the importance of generating enough MC events to estimate the huge backgrounds at a 100 TeV pp collider.

Additionally, we found that the reach for both strategies is considerably reduced when the difference $\mu - M_1$ is high, since it results in a highly boosted h that decays to a collimated pair of b -jets that will most likely be identified as a single jet. This is not an insurmountable difficulty - there are ways to deal with collimated jets, although they are beyond the scope of this work. This issue does, however, highlight the necessity of improving isolation performance at a 100 TeV pp machine, where large mass hierarchies can result in highly boosted/collimated decay products. For a review of currently used methods to determine jet substructure, see [41]. In the future, machine learning techniques might be profitably applied to this area as well - for a review of developments along this line, see [42].

The collimation of the b jets, along with the fact that we simulate detector effects using Delphes, result in a relatively lower reach in the high μ , low M_1 region than the multilepton analysis in [16], which is able to exclude Higgsinos up to a mass of 2.8 TeV for massless Binos, or discover them up to a mass of 1.8 TeV. However, the reach of our analysis is higher in the region where the difference between μ and M_1 is smaller. This is consistent with our usage of the razor variable M_R , which is sensitive to the mass difference between the parent Higgsinos and the daughter Bino.

A 100 TeV pp collider represents an excellent opportunity to discover physics beyond the Standard Model. The extremely high energies and luminosities involved will present new challenges for particle physicists, and it is likely that machine learning will play an important part in facing them.

Acknowledgments

We would like to thank Matt Leone and Ken Johns for helpful discussions. The research activities of AP and SS were supported in part by the Department of Energy under Grant DE-FG02-13ER41976/de-sc0009913. An allocation of computer time from the UA Research Computing High Performance Computing (HPC) and High Throughput Computing (HTC) at the University of Arizona is gratefully acknowledged. We also thank KITP for its hospitality when this draft is completed. This research was supported in part by the National Science Foundation under Grant No. NSF PHY-1748958.

References

- [1] S. P. Martin, *A Supersymmetry Primer*, [hep-ph/9709356](https://arxiv.org/abs/hep-ph/9709356).

- [2] G. Bertone, D. Hooper and J. Silk, *Particle dark matter: Evidence, candidates and constraints*, *Phys. Rept.* **405** (2005) 279 [[hep-ph/0404175](#)].
- [3] ATLAS collaboration, *Search for new phenomena using the invariant mass distribution of same-flavour opposite-sign dilepton pairs in events with missing transverse momentum in $\sqrt{s} = 13$ TeV pp collisions with the ATLAS detector*, *Eur. Phys. J.* **C78** (2018) 625 [[1805.11381](#)].
- [4] CMS collaboration, *Search for natural and split supersymmetry in proton-proton collisions at $\sqrt{s} = 13$ TeV in final states with jets and missing transverse momentum*, *JHEP* **05** (2018) 025 [[1802.02110](#)].
- [5] J. D. Wells, *Implications of supersymmetry breaking with a little hierarchy between gauginos and scalars*, in *11th International Conference on Supersymmetry and the Unification of Fundamental Interactions (SUSY 2003) Tucson, Arizona, June 5-10, 2003*, 2003, [[hep-ph/0306127](#)].
- [6] N. Arkani-Hamed, S. Dimopoulos, G. F. Giudice and A. Romanino, *Aspects of split supersymmetry*, *Nucl. Phys.* **B709** (2005) 3 [[hep-ph/0409232](#)].
- [7] G. F. Giudice and A. Romanino, *Split supersymmetry*, *Nucl. Phys.* **B699** (2004) 65 [[hep-ph/0406088](#)].
- [8] CMS COLLABORATION collaboration, *Searches for new phenomena in events with jets and high values of the M_{T2} variable, including signatures with disappearing tracks, in proton-proton collisions at $\sqrt{s} = 13$ TeV*, Tech. Rep. CMS-PAS-SUS-19-005, CERN, Geneva, 2019.
- [9] ATLAS COLLABORATION collaboration, *SUSY July 2019 Summary Plot Update*, Tech. Rep. ATL-PHYS-PUB-2019-022, CERN, Geneva, Jul, 2019.
- [10] CMS collaboration, *Search for electroweak production of charginos and neutralinos in multilepton final states in proton-proton collisions at $\sqrt{s} = 13$ TeV*, *JHEP* **03** (2018) 166 [[1709.05406](#)].
- [11] ATLAS collaboration, *Search for pair production of higgsinos in final states with at least three b-tagged jets in $\sqrt{s} = 13$ TeV pp collisions using the ATLAS detector*, Submitted to: *Phys. Rev.* (2018) [[1806.04030](#)].
- [12] CMS collaboration, *Combined search for electroweak production of charginos and neutralinos in proton-proton collisions at $\sqrt{s} = 13$ TeV*, *JHEP* **03** (2018) 160 [[1801.03957](#)].
- [13] ATLAS collaboration, *Search for supersymmetry in events with four or more leptons in $\sqrt{s} = 13$ TeV pp collisions with ATLAS*, [1804.03602](#).
- [14] T. Han, S. Padhi and S. Su, *Electroweakinos in the Light of the Higgs Boson*, *Phys. Rev.* **D88** (2013) 115010 [[1309.5966](#)].
- [15] B. S. Acharya, K. Bozek, C. Pongkitivanichkul and K. Sakurai, *Prospects for observing charginos and neutralinos at a 100 TeV proton-proton collider*, *JHEP* **02** (2015) 181 [[1410.1532](#)].
- [16] S. Gori, S. Jung, L.-T. Wang and J. D. Wells, *Prospects for Electroweakino Discovery at a 100 TeV Hadron Collider*, *JHEP* **12** (2014) 108 [[1410.6287](#)].
- [17] N. Arkani-Hamed, T. Han, M. Mangano and L.-T. Wang, *Physics opportunities of a 100 TeV proton-proton collider*, *Phys. Rept.* **652** (2016) 1 [[1511.06495](#)].

- [18] M. Benedikt and F. Zimmermann, “Future Circular Collider Study, Status and Progress.” https://indico.cern.ch/event/550509/contributions/2413230/attachments/1396002/2128079/170116-MBE-FCC-Study-Status_ap.pdf, 2017.
- [19] CEPC-SPPC Study Group, “CEPC-SPPC Preliminary Conceptual Design Report. 1. Physics and Detector.” <http://cepc.ihep.ac.cn/preCDR/volume.html>, 2015.
- [20] R. Contino et al., *Physics at a 100 TeV pp collider: Higgs and EW symmetry breaking studies*, 2016.
- [21] T. Golling et al., *Physics at a 100 TeV pp collider: beyond the Standard Model phenomena*, 2016.
- [22] M. Mangano et al., *Physics at a 100 TeV pp collider: Standard Model processes*, 2016.
- [23] M. Low and L.-T. Wang, *Neutralino dark matter at 14 TeV and 100 TeV*, *JHEP* **08** (2014) 161 [[1404.0682](#)].
- [24] G. Grilli di Cortona, *Hunting electroweakinos at future hadron colliders and direct detection experiments*, *JHEP* **05** (2015) 035 [[1412.5952](#)].
- [25] M. Cirelli, F. Sala and M. Taoso, *Wino-like Minimal Dark Matter and future colliders*, *JHEP* **10** (2014) 033 [[1407.7058](#)].
- [26] R. Mahbubani and J. Zurita, *Probing compressed dark sectors at 100 TeV in the dileptonic mono-Z channel*, *Submitted to: JHEP* (2018) [[1806.08310](#)].
- [27] T. Han, S. Mukhopadhyay and X. Wang, *Electroweak Dark Matter at Future Hadron Colliders*, [1805.00015](#).
- [28] C. Rogan, *Kinematical variables towards new dynamics at the LHC*, 2010.
- [29] ATLAS collaboration, *Observation of a new particle in the search for the Standard Model Higgs boson with the ATLAS detector at the LHC*, *Phys. Lett.* **B716** (2012) 1 [[1207.7214](#)].
- [30] CMS collaboration, *Observation of a new boson at a mass of 125 GeV with the CMS experiment at the LHC*, *Phys. Lett.* **B716** (2012) 30 [[1207.7235](#)].
- [31] J. Bramante, P. J. Fox, A. Martin, B. Ostdiek, T. Plehn, T. Schell et al., *Relic Neutralino Surface at a 100 TeV Collider*, *Phys. Rev.* **D91** (2015) 054015 [[1412.4789](#)].
- [32] A. Berlin, T. Lin, M. Low and L.-T. Wang, *Neutralinos in Vector Boson Fusion at High Energy Colliders*, *Phys. Rev.* **D91** (2015) 115002 [[1502.05044](#)].
- [33] W. Beenakker, M. Klasen, M. Kramer, T. Plehn, M. Spira and P. M. Zerwas, *The Production of charginos / neutralinos and sleptons at hadron colliders*, *Phys. Rev. Lett.* **83** (1999) 3780 [[hep-ph/9906298](#)].
- [34] A. Djouadi, M. M. Muhlleitner and M. Spira, *Decays of supersymmetric particles: The Program SUSY-HIT (SUSpect-SdecaY-Hdecay-InTerface)*, *Acta Phys. Polon.* **B38** (2007) 635 [[hep-ph/0609292](#)].
- [35] PARTICLE DATA GROUP collaboration, *Review of Particle Physics*, *Chin. Phys.* **C40** (2016) 100001.
- [36] J. Alwall, R. Frederix, S. Frixione, V. Hirschi, F. Maltoni, O. Mattelaer et al., *The automated computation of tree-level and next-to-leading order differential cross sections, and their matching to parton shower simulations*, *JHEP* **07** (2014) 079 [[1405.0301](#)].

- [37] T. Sjostrand, S. Mrenna and P. Z. Skands, *PYTHIA 6.4 Physics and Manual*, *JHEP* **05** (2006) 026 [[hep-ph/0603175](#)].
- [38] DELPHES 3 collaboration, *DELPHES 3, A modular framework for fast simulation of a generic collider experiment*, *JHEP* **02** (2014) 057 [[1307.6346](#)].
- [39] E. Conte, B. Fuks and G. Serret, *MadAnalysis 5, A User-Friendly Framework for Collider Phenomenology*, *Comput. Phys. Commun.* **184** (2013) 222 [[1206.1599](#)].
- [40] F. Pedregosa and G. Varoquaux, *Scikit-learn: Machine learning in Python*, *Journal of Machine Learning Research* **12** (2011) 2825 [[1201.0490v2](#)].
- [41] J. Shelton, *Jet Substructure*, in *Proceedings, Theoretical Advanced Study Institute in Elementary Particle Physics: Searching for New Physics at Small and Large Scales (TASI 2012): Boulder, Colorado, June 4-29, 2012*, pp. 303–340, 2013, [1302.0260](#), [DOI](#).
- [42] A. Schwartzman, M. Kagan, L. Mackey, B. Nachman and L. De Oliveira, *Image Processing, Computer Vision, and Deep Learning: new approaches to the analysis and physics interpretation of LHC events*, *J. Phys. Conf. Ser.* **762** (2016) 012035.